

FIRST MEASUREMENT OF $\Gamma(D^{*+})$

M. DUBROVIN

*Wilson Laboratory, Cornell University / Wayne State University
Ithaca, NY 14853, USA
(on behalf of CLEO Collaboration)*

We have made the first measurement of the D^{*+} width using 9/fb of e^+e^- data collected near the $\Upsilon(4S)$ resonance by the CLEO II.V detector. Our method uses advanced tracking techniques and a reconstruction method that takes advantage of the small vertical size of the CESR beam spot to measure the energy release distribution from the $D^{*+} \rightarrow D^0\pi^+$ decay. Our preliminary result is $\Gamma(D^{*+}) = 96 \pm 4$ (Statistical) ± 22 (Systematic) keV.

A measurement of $\Gamma(D^{*+})$ opens an important window on the non-perturbative strong physics involving heavy quarks. The basic framework of the theory is well understood, however, there is still much speculation - predictions for the width range from 15 keV to 150 keV¹. We know the D^{*+} width is dominated by strong decays, since the measured magnetic-dipole transition rate is small, $Br(D^{*+} \rightarrow D^+\gamma) = 1.68 \pm 0.45\%$,² and can be neglected to the first order. The level splitting in the B sector is not large enough to allow real strong transitions. Therefore, a measurement of the D^{*+} width gives unique information about the strong coupling constant in heavy-light systems³, $g_{D^*D\pi}$ or g .

Prior to this measurement, the D^{*+} width was limited to be less than 131 keV at the 90% confidence level by the ACCMOR collaboration⁴. The limit was based on 110 signal events reconstructed in two D^0 decay channels with a background of 15% of the signal. This contribution describes a measurement of the D^{*+} width with the CLEO II.V detector where the signal, in excess of 11,500 events, is reconstructed through a single, well-measured sequence, $D^{*+} \rightarrow \pi_{\text{slow}}^+ D^0$, $D^0 \rightarrow K^-\pi^+$. Consideration of charge conjugated modes are implied throughout this paper. The level of background under the signal is less than 3% in our loosest selection.

The CLEO detector has been described in detail elsewhere. All of the data used in this analysis are taken with the detector in its II.V configuration⁵. The data were taken in symmetric e^+e^- collisions at a center of mass energy around 10 GeV with an integrated luminosity of 9.0/fb provided by the Cornell Electron-positron Storage Ring (CESR). The nominal sample follows the selection of $D^{*+} \rightarrow \pi_{\text{slow}}^+ D^0 \rightarrow \pi_{\text{slow}}^+ K^-\pi^+$ candidates used in our $D^0 - \bar{D}^0$ mixing analysis⁶.

Our reconstruction method takes advantage of the small CESR beam spot and the kinematics and topology of the $D^{*+} \rightarrow \pi_{\text{slow}}^+ D^0 \rightarrow \pi_{\text{slow}}^+ K^-\pi^+$ decay chain. The K^- and π^+ are required to form a common vertex. The resultant D^0 candidate momentum vector is then projected back to the CESR luminous region to determine the D^0 production point. The CESR luminous region has a Gaussian width $\sim 10 \mu\text{m}$ vertically and $\sim 300 \mu\text{m}$ horizontally. This procedure determines an accurate D^0 production point. Then the π_{slow}^+ track is re-fit constraining its

trajectory to intersect the D^0 production point. This improves the resolution on the energy release, Q , by more than 30% over simply forming the appropriate invariant masses of the tracks. The improvement to resolution is essential to our measurement of the width of the D^{*+} . Our resolution is shown in Figure 1 and is typically 150 keV. The good agreement reflects that the kinematics and sources of errors on the tracks, such as number of hits and the effects of multiple scattering in detector material, are well modeled.

The challenge of measuring of the D^{*+} width is understanding the tracking system response function since the experimental resolution exceeds the width we are trying to measure. We depend on exhaustive comparisons between a GEANT⁷ based detector simulation and our data. We addressed the problem by selecting samples of candidate D^{*+} decays using three strategies. First we produced the largest sample from data and simulation by imposing only basic tracking consistency requirements. We call this the *nominal* sample. Second we refine the nominal sample selecting candidates with the best measured tracks by making very tight cuts on tracking parameters. There is special emphasis on choosing those tracks that are well measured in our silicon vertex detector. This reduces our nominal sample by a factor of thirty and, according to our simulation, has negligible contribution from tracking mishaps. We call this the *tracking selected* sample. A third alternative is to select our data on specific kinematic properties of the D^{*+} decay that minimize the dependence of the width of the D^{*+} on detector mismeasurements. The nominal sample size is reduced by a factor of three and a half and, again according to our simulation, the effect of tracking problems is reduced to negligible levels. We call this the *kinematic selected* sample. Table 1 summarizes the statistics in our three samples.

In all three samples the width is extracted with an unbinned maximum likelihood fit to the energy release, $Q = m(K^-\pi^+\pi_{\text{slow}}^+) - m(K^-\pi^+) - m_{\pi^+}$, distribution and compared with the simulation's generated value to determine a bias which is then applied to the data. The three different samples yield consistent values for the width of the D^{*+} giving us confidence that our simulation accurately models our data.

We assume that the intrinsic width of the D^0 is negligible, $\Gamma(D^0) \ll \Gamma(D^{*+})$, implying that the observed width of Q distribution is dominated by the shape given by the D^{*+} intrinsic width and the tracking system response function. Thus we consider the pairs of Q_i and σ_{Q_i} for $D^{*+} \rightarrow \pi_{\text{slow}}^+ D^0 \rightarrow \pi_{\text{slow}}^+ K^-\pi^+$ where σ_{Q_i} is given for each i -th candidate by propagating the tracking errors in the kinematic fit of the charged tracks⁸. We perform an unbinned maximum likelihood fit to the Q distribution, minimizing the likelihood function

$$L = 2(N_s + N_b) - 2 \sum_{i=1}^N \log[N_s \cdot S(Q_i, \sigma_{Q_i}; \Gamma_0, Q_0, f_{\text{mis}}, \sigma_{\text{mis}}) + N_b \cdot B(Q_i; b_{1,2,3})], \quad (1)$$

where S and B are respectively the signal and the background shapes, N_s and N_b number of signal and background events.

The shape of the underlying signal is assumed to be given by a P-wave Breit-Wigner, with central value of Q , Q_0 . We considered a relativistic and a non-relativistic Breit-Wigners as a model of the underlying signal shape, and found negligible difference in the fit parameters. The width of the Breit-Wigner depends on Q and is given by

$$\Gamma(Q) = \Gamma_0 \left(\frac{P}{P_0} \right)^3 \left(\frac{m_0}{m} \right)^2, \quad (2)$$

where Γ_0 is equivalent to $\Gamma(D^{*+})$, m and P are the measured candidate D^{*+} mass and π_{slow}^+ or D^0 momentum in the D^{*+} rest frame and P_0 and m_0 are the values computed using Q_0 . The effect of the mass term is negligible at our energy. The partial width and the total width differ negligibly in their dependence on Q for $Q > 1 \text{ MeV}$. We use Eqn 2 suitably normalized to describe of Q effects on width.

Table 1: Summary of our data sample, simulation biases, and fit results.

Parameter	Sample		
	Nominal	Tracking	Kinematic
Candidates	11496	368	3284
Background Fraction (%)	2.51 ± 0.27	4.1 ± 1.9	4.05 ± 0.49
$\Gamma_{\text{fit}} - \Gamma_{\text{generated}}$ (keV)	2.7 ± 2.1	1.7 ± 6.4	4.3 ± 3.1
Fit Γ_0 (keV)	98.9 ± 4.0	106.0 ± 19.6	108.1 ± 5.9
D^{*+} Width (keV)	96.2 ± 4.0	104 ± 20	103.8 ± 5.9

Table 2: Results of the fits described in the text. The uncertainties are statistical.

Parameter	Sample		
	Nominal	Tracking	Kinematic
Γ_0 (keV)	98.9 ± 4.0	106.0 ± 19.6	108.1 ± 5.9
Q_0 (keV)	5853 ± 2	5854 ± 10	5850 ± 4
N_s	11207 ± 109	353 ± 20	3151 ± 57
f_{mis} (%)	5.3 ± 0.5	NA	NA
σ_{mis} (keV)	508 ± 39	NA	NA
N_b	289 ± 31	15 ± 7	133 ± 16

For each candidate the signal shape, S , is a convolution of the Breit-Wigner function with a resolution Gaussian with width, σ_{Qi} , determined by the tracking errors, as a model of our finite resolution. Figure 1 shows the distribution of σ_Q for the data and the simulation. We allow a small fraction of the signal, f_{mis} , to be parameterized by a single Gaussian with effective resolution, σ_{mis} , different from measured, σ_{Qi} . This shape is included in the fit to model the tracking mishaps, mis-assigned hits and hard multiple scatters, which our simulation predicts to be at the 5% level in the nominal sample and negligible in both the tracking and kinematic selected samples. For the purpose of systematic study the σ_Q has a scale factor, k , which is fixed to one in our nominal fits.

The fit also includes a background contribution with fixed shape, B , presented by polynomial function with three or more parameters, $b_{1,2,3}$. This shape is taken from fits to the background prediction of our simulation. The level of the background is allowed to float in our standard fit.

The fitter has been extensively tested both numerically and with input from our full simulation. We find that the fitter performs reliably giving normal distributions for the floating parameters and their uncertainties. It also reproduces the input $\Gamma(D^{*+})$ from 0 to 130 keV with offset consistent with zero, as shown in Table 1.

We note that if all the parameters are allowed to vary simultaneously there is strong correlation among the intrinsic width Γ_0 , the fraction of mismeasured events f_{mis} , and the σ_Q scale factor k , as one would expect. Thus our nominal fit holds k fixed to one, but in our systematic studies we either fix one of the three or provide a constraint with a contribution to the likelihood if the parameter varies from its nominal value.

Figures 2, 3, and 4 respectively display the fit to the nominal, tracking, and kinematic selected data samples. The results of the fits are summarized in Table 2. Correlations among the floating parameters of the fit are negligible.

Figure 5 displays the likelihood as a function of the width of the D^{*+} for the fits to the three data samples.

The agreement is excellent among the fits to three sample, and when the offsets are applied we obtain D^{*+} widths listed in the last row in Table 1. The indicated uncertainties are only statistical.

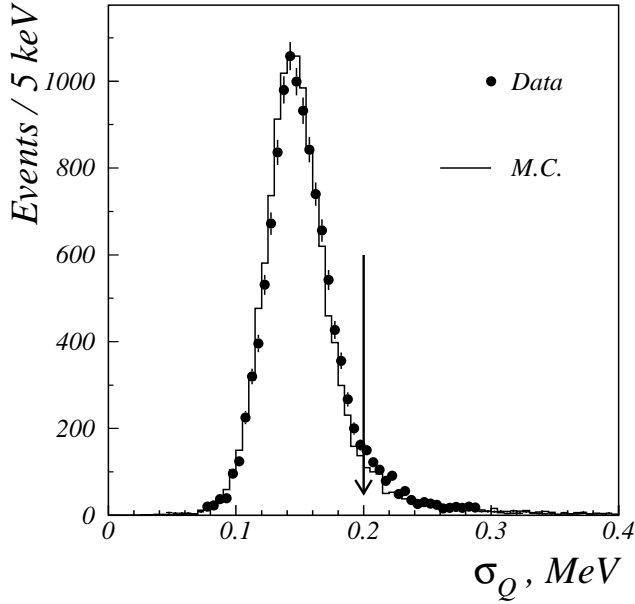


Figure 1: Distribution of σ_Q , the uncertainty on Q as determined from propagating track fitting errors. The arrow indicates a selection cut.

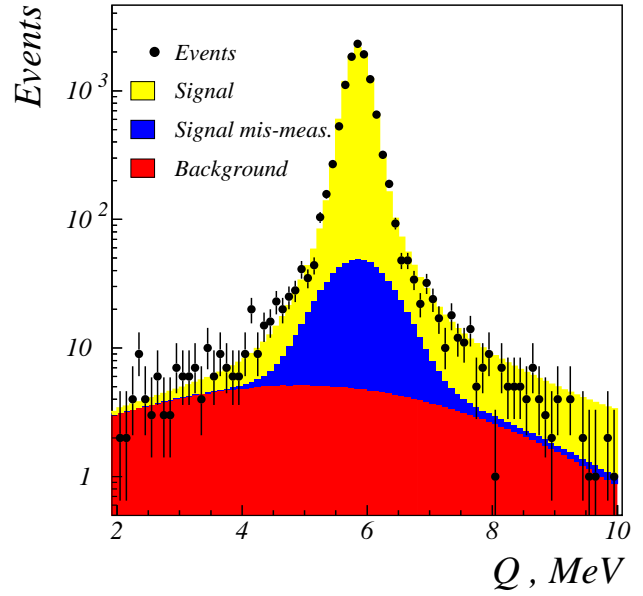


Figure 2: Fit to *nominal* data sample. The different contributions to the fit are shown by different colors.

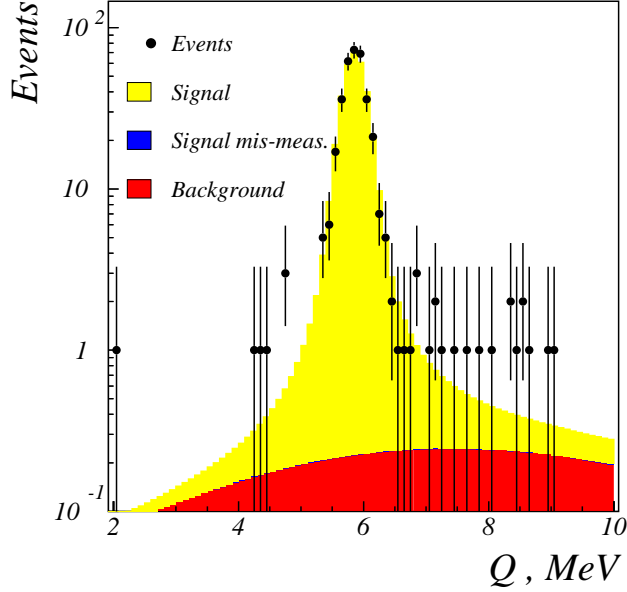


Figure 3: Fit to *tracking selected* data sample.

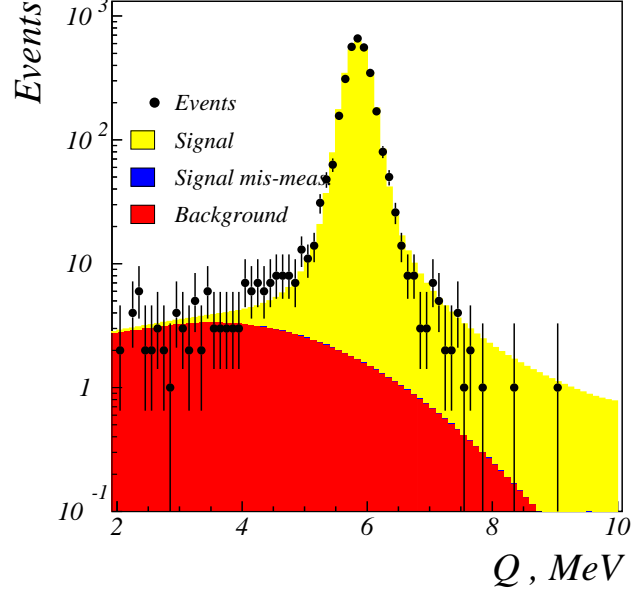


Figure 4: Fit to *kinematic selected* data sample.

We discuss the sources of systematic uncertainties on our measurements of the width of the D^{*+} in the order of their size. The most important contribution is the variation of the result as a function of the kinematic parameters of the D^{*+} decay. The next most important contribution comes from any mismodeling of σ_Q 's dependence on the kinematic parameters. We take into account correlations among the less well measured parameters of the fit, such as k , f_{mis} , and σ_{mis} , by fixing each parameter at ± 1 standard deviation from their central fit values, repeating

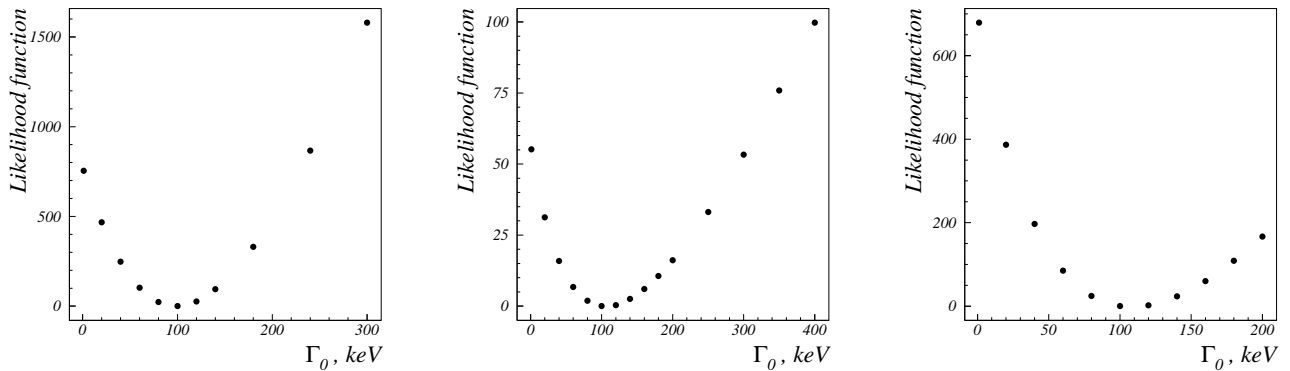


Figure 5: Likelihood function versus measured D^{*+} width for the nominal (left), tracking (center), and kinematic (right) selected data samples.

Table 3: Systematic uncertainties on the width of the D^{*+} and Q_0

Source	Uncertainties in keV					
	Sample					
	Nominal		Tracking		Kinematic	
	$\delta\Gamma(D^{*+})$	δQ_0	$\delta\Gamma(D^{*+})$	δQ_0	$\delta\Gamma(D^{*+})$	δQ_0
Running of Q	16	15	16	15	16	15
Mismodeling of σ_Q	11	< 1	9	4	7	< 1
Fit Correlations	8	3	9	4	9	5
Vertex Reconstruction	4	2	4	2	4	2
Background Shape	4	< 1	2	< 1	2	< 1
Offset Correction	2	NA	6	NA	3	NA
Data Digitization	1	1	1	1	1	1
Quadratic Sum	22	15	22	16	20	16

the fit, and adding in quadrature the variation in the width of the D^{*+} and Q_0 from their central values. We have studied in the simulation the sources of mismeasurement that give rise to the resolution on the width of the D^{*+} by replacing the measured values with the generated values for various kinematic parameters of the decay products. We have then compared these uncertainties with analytic expressions for the uncertainties. The only source of resolution that we cannot account for in this way is a small distortion of the kinematics of the event caused by the algorithm used to reconstruct the D^0 origin point described above. We consider uncertainties from the background shape by allowing the coefficients of the background polynomial to float. Minor sources of uncertainty are from the width offsets derived from our simulation, and our data storage digitization resolution of 1 keV.

An extra and dominant source of uncertainty on Q_0 is the energy scale of our measurements. We are still evaluating the size of this contribution.

Table 3 summarizes the systematic uncertainties on the width of the D^{*+} and Q_0 .

In summary we have measured the width of the D^{*+} by studying the distribution of the energy release in $D^{*+} \rightarrow D^0\pi^+$ followed by $D^0 \rightarrow K^-\pi^+$ decay. With our estimate of the systematic uncertainties for each of the three samples being essentially the same we chose to report the result for the sample with the smallest statistical uncertainty, the minimally selected sample, and obtain

$$\Gamma(D^{*+}) = 96 \pm 4 \pm 22 \text{ keV}, \quad (3)$$

where the first uncertainty is statistical and the second is systematic.

This preliminary measurement is the first of the width of the D^{*+} , and corresponds to a strong coupling constants³

$$g = 0.59 \pm 0.01 \pm 0.07 \quad \text{or} \quad g_{D^*D\pi} = 17.9 \pm 0.3 \pm 1.9. \quad (4)$$

This is consistent with theoretical predictions based on HQET and relativistic quark models, but higher than predictions based on QCD sum rules and lattice calculations.

Acknowledgments

We thank I.I. Bigi, A. Khodjamirian, and P. Singer for valuable discussions. We gratefully acknowledge the effort of the CESR staff in providing us with excellent luminosity and running conditions. M. Selen thanks the PFF program of the NSF and the Research Corporation, and A.H. Mahmood thanks the Texas Advanced Research Program. This work was supported by the National Science Foundation, the U.S. Department of Energy, and the Natural Sciences and Engineering Research Council of Canada.

References

1. Belyaev et al. *Phys. Rev. D* **51**, 6177 (1995). contains a recent survey summarizing and referencing previous theoretical work. P. Singer, *Acta Phys. Polon.* B30 3849 (1999), J.L. Goity and W. Roberts JLAB-THY-00-45, hep-ph/0012314, and M. Di Pierro and E. Eichten, hep-ph/0104208 appear since that survey.
2. J. Bartelt *et al.* (CLEO Collaboration), *Phys. Rev. Lett.* **80**, 3919 (1998).
3. M. Wise, *Phys. Rev. D* **45**, R2188 (1992).
4. S. Barlag *et al.*, *Phys. Lett. B* **278**, 480 (1992).
5. Y. Kubota *et al.*, (CLEO Collaboration), *Nucl. Instrum. Methods A* **320**, 66 (1992); T. Hill, *Nucl. Instrum. Methods A* **418**, 32 (1998).
6. R. Godang *et al.* (CLEO Collaboration), *Phys. Rev. Lett.* **84**, 5038 (2000).
7. R. Brun *et al.*, GEANT3 Users Guide, CERN DD/EE/84-1.
8. P. Billior, *Nucl. Instrum. Methods A* **225**, 352 (1984).